EXHAUST NOISE ANALYSIS RESEARCH FOR A SINGLE-CYLINDER DIESEL ENGINE AND EVALUATION OF NOISE FILTRATION BY SIMULATION
/
STUDII ŞI CERCETĂRI PRIVIND ZGOMOTUL DE EVACUARE PENTRU UN MOTOR DIESEL MONOCILINDRIC ŞI EVALUAREA FILTRĂRII ZGOMOTULUI PRIN SIMULARE

Golgot Claudiu[*1)]; Filip Nicolae[1)] [1]
Faculty of Road Vehicles, Mechatronics and Mechanics, Technical University of Cluj–Napoca / Romania
Tel: 0765429645; E-mail: golgot_claudiu@yahoo.com
DOI: https://doi.org/10.35633/inmateh-65-21

Keywords: *acoustic, exhaust noise, diesel engine, filter, audio*

ABSTRACT

The paper develops an analysis of exhaust noise for a single-cylinder diesel engine tested in laboratory conditions. The acoustic signal at the engine exhaust system, for the speed range 1,300 – 2,700 rpm was measured and recorded. The results of the noise recordings were subjected to a processing from which the variation of the noise level depending on the engine speed was obtained. Next, the physiological effect of acoustic filtrations for noise recordings was analyzed by simulation. This allowed the optimization of the exhaust noise, having identified the areas and the optimal attenuation effect. In the performed simulations, it was found that the low frequencies require the highest attenuation background.

REZUMAT

Lucrarea dezvoltă o analiză a zgomotului de evacuare pentru un motor diesel monocilindric testat în condiții de laborator. Semnalul acustic este măsurat și înregistrat la evacuarea motorului pentru intervalul variat de turații cuprins între 1.300 - 2.700 rpm. Măsurătorile de zgomot au fost supuse unor prelucrări acustice din care a rezultat variația nivelului de zgomot în funcție de viteza motorului. Efectul fiziologic al filtrărilor acustice a fost analizat prin simulări audio. Acest lucru a permis optimizarea zgomotului de evacuare, identificându-se zonele și efectul de atenuare optimă. Prin simulările efectuate, am constatat că nivelul de joasă frecvență necesită cea mai mare atenuare.

INTRODUCTION

Any pollutant that exceeds normal tolerance or absorption limits is a risk factor for the environment and human health. After the chemical pollution of the air, the noise produced by traffic is the most harmful pollutant in the urban environment (*Colin, 2017*). Exhaust noise is the main source of noise in internal combustion engines representing a percentage of 20% (*Filip, 2000; Matthew, 2004*).

Methods for reducing exhaust noise (*Peter et al., 2015*) by using an attenuator with an adaptable (flexible) internal structure were analyzed. This design allows the control of the acoustic waves according to the engine's functioning variations. With this type of attenuator, it achieved a transmission loss higher than 10 dB in the selected frequency band.

Another noise attenuation analysis using the transmission attenuation method is presented by numerical simulation of a circular attenuator (*Wael A, 2020; Wei and Li, 2016*). This type of attenuator consists of a resonance chamber and a perforated tube. In this case increasing the exhaust gas flow generally increases the transmission attenuation property and decreases the amplitude of the resonant frequency.

Similarly, to improve the performance of an attenuator mounted to the exhaust of a diesel engine, software simulation was studied and compared to experimental laboratory measurements (*Jung et al., 2015*). The conclusion was that for the frequency range less than 3,000 Hz the error level between software simulation and physical measurements is very small.

For a minimal influence on the internal combustion engine power, it was analyzed an attenuator with a volume six times larger than the volume of the engine cylinder, a diameter of two and a half times the diameter of the exhaust pipe and a length of four times the size of the diameter (*Babu and Amba, 2014*).

[1] *Golgot Claudiu, Ph.D. Stud.; Filip Nicolae, Prof. M.S. Eng*

In the attenuation calculation, the attenuator was equipped with a series of perforated plates of different properties. This type of simulations was performed avoiding the natural resonance frequency of the system, thus obtaining attenuation from 86.77 dB to 74.44 dB.

In an analysis of the exhaust noise level and the back pressure level (*Mohiuddin et al., 2005*), according to various constructive forms of the attenuator, results that the back pressure level is the difference between the exhaust pipe pressure and the atmospheric pressure. Concluding, the number of components (pipes, resonating chambers and perforated orifices) directly influences the flow of exhaust gases through the attenuator. High noise level attenuation means high back pressure, thus influencing the performance of the engine, which is undesirable. For this reason, a sizing calculation is necessary considering the low, medium and high frequency range.

Generally, the most common attenuators used to reduce attenuation noise are composed of several resonant chambers (reactive type). The characteristics of these types of resonators are well presented in the acoustic literature (*Munjal, 2014*). Further reducing exhaust noise and improving fuel consumption are also proposed in studies using an electromagnetic audio speaker as a noise generator (Rossi, 2002). Changing the dimensions of the resonant chambers changes the resonant frequency and the amplitude of pressure in the resonator cavity (*Myonghyon, 2008*).

A theoretical calculation analysis predicting the attenuation of acoustic intensity by transmission loss (TL) uses the transfer matrix method (TMM) compared to experimental tests (*Mihai and Ovidiu, 2006*). For the experimental testing of the acoustic transmission loss (TL) of the attenuator in the absence of a noise generated by the exhaust gas, the stand is composed of equipment's such as: audio signal generator; signal power amplifier; omnidirectional audio speakers; capacitive microphones; data acquisition board and data storage unit, computer (PC).

According to experimental tests the mathematical model does not show major differences (except for certain areas of the frequency spectrum) so it can be considered a reliable method in calculating noise attenuators. The acoustic behavior of a double-chamber circular exhaust system and its effects depends on various changes such as the attenuator material, the number of resonant chambers and their size (*Erkan et al., 2021; Selamet et al., 2003*). In this situation, the acoustic attenuation performance can be significantly improved because of these effects.

Similarly, an optimization study of an attenuator composed of several resonant chambers positioned in a cascade, each with different characteristic properties of transmission loss (TL) was analyzed (*Lee J. et al., 2020; Xiang Yu et al., 2015; Fang et al., 2009*). To improve the level of attenuation (TL) from the perspective of increasing the frequency range in the operation of the attenuator, an analysis on the effect of changing the internal geometric parameters compared to the initial stage is presented. Also, in this case the test stand consists of a pulse generator speaker, a power amplifier, piezoelectric microphones, data acquisition board, computer unit (PC) and cone-shaped sound-absorbing material at the end of the piping.

In this paper, it is aimed at developing a method for identifying the characteristic of exhaust noise measured in a single-cylinder diesel engine and presenting a technique for optimizing it by simulation. The novelty of the research lies in the fact that a simulation of the noise filtrations was performed compared to the physiological audio effect. Also, the identification of frequencies to attenuate the sound pressure level is the basic information necessary to design efficient noise attenuators.

MATERIALS AND METHODS

Noise measurements were performed on the exhaust system of a single-cylinder diesel engine code KM186FA (four stroke, P_{max} = 5.7 kW / 3,000 rpm), without a noise attenuation system attached, for a wide range of engine speeds at-load free mode. All measurements are in linear frequency bands without acoustic weighting. The value of the engine speed was measured using a digital laser tachometer with a tolerance of 1%. The equipment used to configure the experimental stand are the computer unit, the Solo-01dB sound level meter. The schematic configuration of the experiment configuration is shown in Fig. 1. The time interval for each measurement (at each engine speed) was 60 seconds. For a comparison check of the equivalent noise level L_{eq}, two acoustic sound level meters, initially calibrated (Solo-01dB and Norsonic-12 equipment) were used. The Solo-01dB equipment allows a more detailed visualization and processing of noise variation in frequency bands.

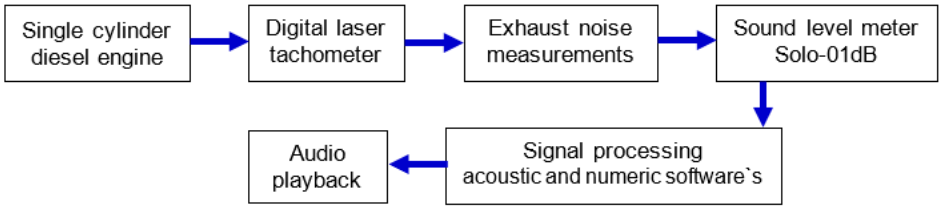

Fig. 1 - Schematic configuration of the experiment setup

The proposed research method requires several stages. These are shown in the block diagram in Fig. 2. The first stage was to collect data by performing noise measurements at the engine exhaust positioning the sound level meters at a distance of 0.5 m, height of 1 m and at 45 ° from the exhaust. The signal was recorded in the real time with a fixed period of 60 seconds set in the sound level meters. The acoustic signal was recorded directly on the PC unit using software specific to the sound level meters. Due to the very large number of recorded values, the signal was processed in several stages (3,072,000 units with a purchase period of 1,953·e-0.5 seconds).

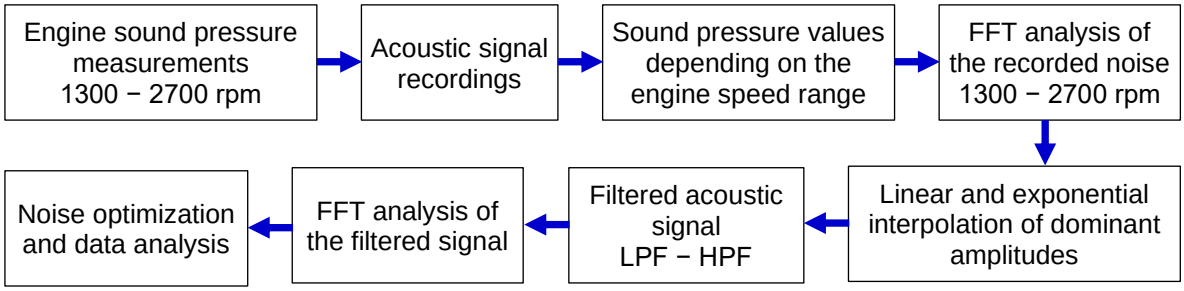

Fig. 2 - Schematic configuration with the main stages of the experiment

The second stage was the decomposition into FFT (Fast Fourier Transform) series where the level of the dominated amplitudes and their occurrence frequencies were determined depending on the engine's speed. Following the results obtained, a calculation of linear and exponential interpolation of the dominant amplitudes of order 1, order 2 and order 3 depending on the engine speed was performed. In the third stage, numerical processing, and acoustic filtration (LPF and HPF) of the recorded acoustic signal were performed, through which the noise-generating components and the resulting physiological effect were determined. For a more detailed analysis, the filtered sound pressure values were also decomposed into FFT series.

In the fourth stage, following the experimental determinations obtained previously, it was achieved attenuation by selectively combining the two types of acoustic filters (LPF and HPF) in frequency bands. From the results, the efficiency of acoustic filters and the possibility of experimental determination of the frequency range, for which the attenuator has the expected efficiency, were identified.

SOUND PRESSURE OF THE EXHAUST NOISE

For a detailed visualization of the acoustic signal recorded following the acoustic measurements, the time required to perform three engine cycles depending on speed was sampled. To determine the value of the sample, Equation (1) was used (Filip and Candale, 2002)

$$\Delta_t = \frac{K}{\frac{n}{60} \cdot \frac{2}{\delta}}, \text{ [sec]} \quad (1)$$

where:

Δ_t is the time interval [sec], K is the number of complete engine cycles (three cycles), δ is the number of engine strokes (four strokes) and n is the measured engine operating speed [rpm].

To calculate the x number of values recorded for three engine cycles from the range of values, the Equation (2) was used

$$x = \Delta_t \cdot f_{aq}, \quad (2)$$

where:

f_{aq} is the acquisition frequency of the sound level meter, for the speeds at which the acoustic signal was recorded (in our case 51,200 values / sec).

The calculated values using Equation (1) and Equation (2) are presented in Table 1 where it can be seen, the time interval calculated for three engine cycles at 2700 rpm is 0.14 seconds.

Table 1

Calculated values, depending on engine speed

Engine Speed [rpm]	1,300	1,600	1,900	2,100	2,400	2,700
Time interval Δt [sec]	0.30	0.24	0.20	0.18	0.15	0.14
Number of value x	15,360	12,288	10,240	9,216	7,680	7,168

RESULTS

Fig. 3a shows the variation of the sound pressure recorded for a calculated interval of 0.14 seconds measured at the evacuation of the single-cylinder engine for the speed of 2,700 rpm (at load-free mode). A maximum sound pressure level of 12 Pa can be observed. Analyzing the variation of the sound pressure level measured at the engine speed stabilized at 2,700 rpm confirmed that three engine cycles were captured and the noise measurements performed are correct. Those three tips represent the reference points corresponding to the opening of the engine exhaust valve. For more details, the complex acoustic signal was decomposed into FFT frequency series for each range of idling engine speeds to determine the dominant frequencies and amplitude level. In Fig. 3b it was represented the level of FFT amplitudes at the speed of 2,700 rpm for the low frequency range (200 Hz) where a maximum value of over 2 Pa resulted. Analyzing the amplitude level, in the low frequency range, a linear increase from 0 to 45 Hz and an exponential decrease with increasing frequency were observed.

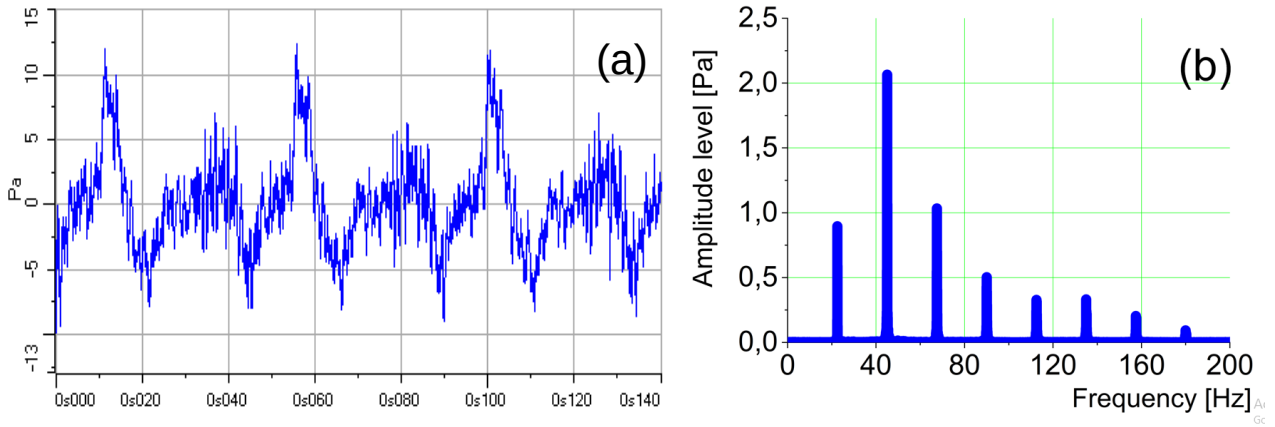

Fig. 3 - Acoustic signal measured at the engine exhaust for the speed range 2,700 rpm
(a) Acoustic pressure for 3 engine cycles, time = 0.14 sec. at load-free mode,
(b) Detailed FFT analysis in the low frequency range

From the FFT analysis, the variation of the first three dominant amplitudes and their frequency of occurrence (Table 2) were extracted. The maximum measured values were obtained at a speed of 2,700 rpm, 2.6 Pa. The acquisition frequency of this sound level meter at which the acoustic signal was recorded is 51,200 values / sec. It is observed how the amplitude level decreases with increasing frequency and the maximum measured values are around frequencies lower than 12,000 Hz. Above the frequency of 16 kHz (ultrasound area) the measured noise is not found in the human audibility zone.

Table 2

Data extracted from the FFT analysis of the acoustic signals recorded at the engine exhaust

Engine Speed [rpm]	**Amplitude order [Pa]**			**Amplitude frequency [Hz]**		
	A_1	A_2	A_3	f_1	f_2	f_3
1,300	0.18	0.40	0.41	13.00	27.00	40.50
1,600	0.17	0.54	0.49	13.50	27.00	41.00
1,900	0.24	0.45	0.68	15.80	31.50	47.30
2,100	0.20	0.44	0.48	17.30	35.00	52.00
2,400	0.46	1.13	0.40	20.00	40.00	60.00
2,700	0.88	2.60	1.03	22.40	45.00	68.00

For the validation of the measurements, identifying the main oscillation frequency of the pressure wave evolving in the exhaust system, derived from Equation (1), depending on the engine speed was calculated by:

$$f_1 = \frac{n \cdot z}{60} \cdot \frac{2}{\delta}, \quad [\text{Hz}] \tag{3}$$

and

$$f_2 = f_1 \cdot 2, \quad [\text{Hz}] \tag{4}$$

where: δ is the number of engine strokes (four strokes), n is measured engine operating speed, z is the number of engine cylinders, f_1 is first degree frequency and f_2 is second degree frequency.

By comparing the measured data values with the calculated values Equation (3, 4) of the first two dominant frequencies (f_1 and f_2), they are almost identical except for the frequencies measured at 1,300 rpm. Thus, it is confirmed that the measurements performed in the laboratory are correct. By mathematical interpolation, the sound pressure level of the first two dominant amplitudes respects an exponential increase with increasing speed (Fig. 4a. and Fig. 4b.). In the case of third order amplitudes (Fig. 4c.) the amplitudes show a very large pressure variation, especially for frequencies between 1,900 Hz and 2,400 Hz, which is why linear or exponential interpolation for third order amplitude cannot be considered.

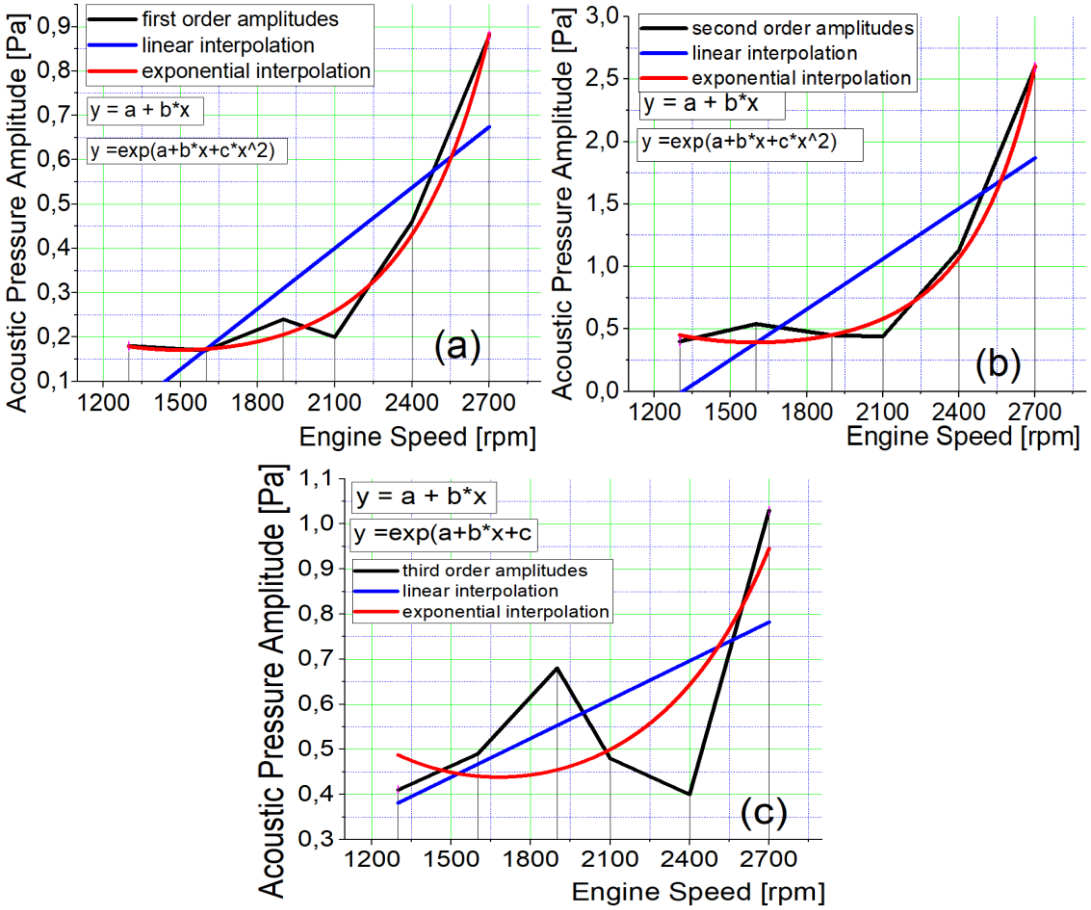

Fig. 4 - Linear and exponential FFT amplitude interpolation, for the dominant frequencies
(a) first order amplitudes, (b) second order amplitudes, (c) third order amplitudes

SIMULATION ANALYSIS OF THE EFFECT OF ACOUSTIC FILTERS

To simulate the effects of acoustic filtering, the initially measured signal and the filtered signal are transformed into a "waveform audio file format ". The acoustic filters used in the simulation are low pass filter LPF for high frequency attenuation and high pass filter HPF for low frequency attenuation. These types of filters were chosen because they are most often used in the field of acoustics. For a more detailed image of the component spectral elements, the obtained pressure values are transformed into a series of FFT type amplitudes. In this case the operating frequencies of the acoustic filters are in the range of 50 Hz – 20,000 Hz depending on the human audibility threshold relative to the low, medium and high frequency range. For low pass filter attenuation LPF shown in Fig. 5a. and Fig. 5b., it can be seen how the number of components of the attenuated signal decreases along with the attenuation frequency.

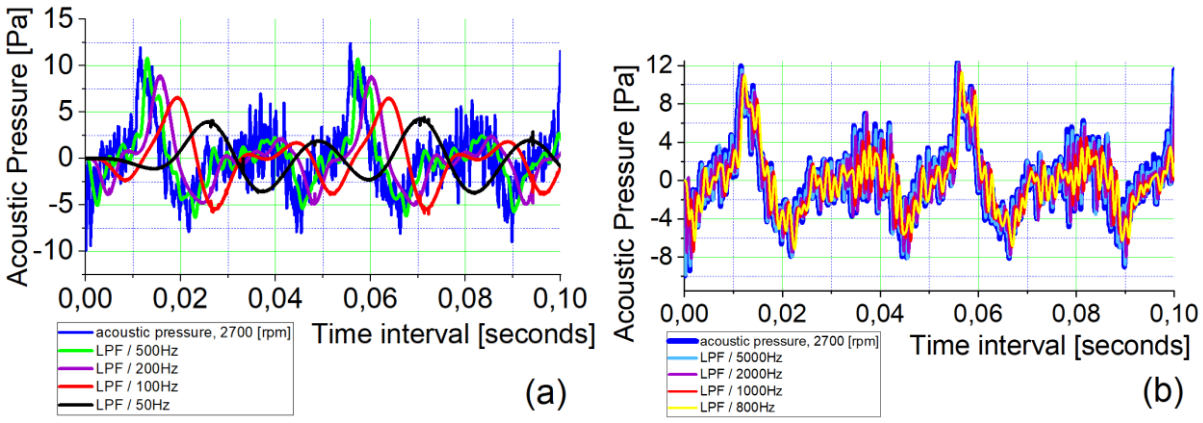

Fig. 5 - Comparison between the sound pressure of the initial signal (2,700 rpm) and the signal filtered by LPF
(a) at 50 Hz, 100 Hz, 200 Hz and 500 Hz, (b)at 800 Hz, 1,000 Hz, 2,000 Hz and 5,000 Hz

After the attenuation LPF by audio playback of the processed signal, from the auditory point of view the perceived noise decreases with the reduction of the attenuation frequency within the limits of the audibility range. For attenuation at 50 Hz, 100 Hz and 200 Hz LPF the noise is difficult to perceive auditorily, but it is present in the form of high amplitude pulsations. These pulsations increase in number of spectral elements as the attenuation frequency increases. After the filters for each attenuation frequency, an FFT type analysis was performed. From this, amplitudes of noise-generating components and their frequency were obtained.

By comparing the FFT analysis of the initial unfiltered signal (Fig. 3b.) and the analysis of the filtered signal by LPF, depending on the actuation frequency (Fig. 6a. and Fig. 6b.), a significant attenuation is observed in the case of 50 Hz filtering. The attenuation of the dominant amplitudes decreases by increasing the actuation frequency.

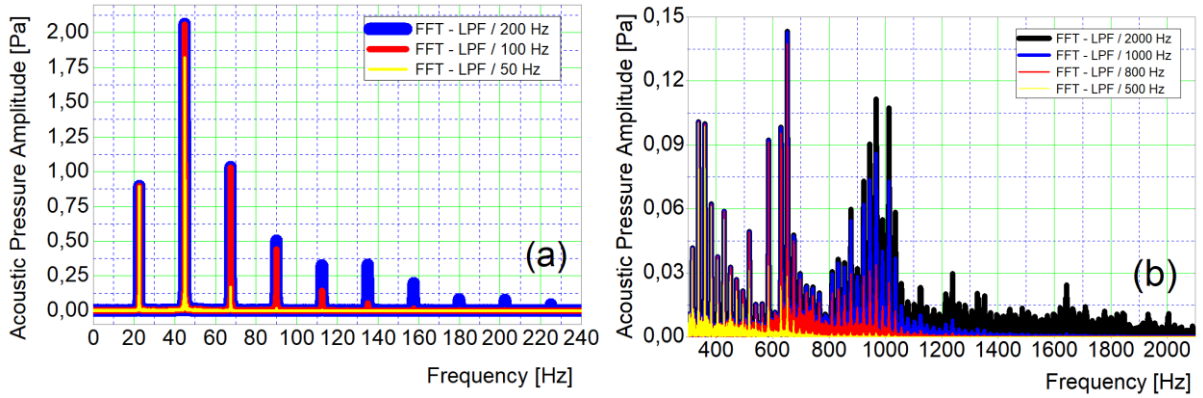

Fig. 6 - FFT diagram of the signal filtered by the LPF method for engine speed of 2,700 rpm
(a) at 50 Hz, 100 Hz and 200 Hz, (b) at 500 Hz, 800 Hz, 1,000 Hz and 2,000 Hz

For the attenuation at 500 Hz LPF, in addition to the pulsations present in the low frequency range, there is a noise specific to internal combustion engines but much lower in intensity. By attenuating at 800 Hz LPF, the perception of the annoying auditory noise begins, being close to the threshold of the painful sensation (120 dB). As the attenuation LPF frequency increases, the noise is composed of an increasing number of component elements (high frequency amplitudes) making it more disturbing auditorily (1,000 Hz, 2,000 Hz, 5,000 Hz, 8,000 Hz, and 10,000 Hz). From the FFT diagrams it can be seen how the acoustic filter LPF works depending on the operating frequency at 500 Hz, 800 Hz, 1,000 Hz and 2,000 Hz. An increase in the number of unfiltered FFT amplitudes can be observed by increasing the actuation frequency. In terms of high frequency LPF works best up to a frequency of 500 Hz. The attenuation effect of the LPF filter above the frequency of 10,000 Hz compared to the initial recorded signal is very difficult to perceive because it approaches the upper limit of the high frequencies heard by the human ear (20 kHz).

In the case of HPF attenuation in Fig. 7a., the number of component elements of the attenuated signal increases with the reduction of the attenuation frequency. From the variation of the acoustic pressure of the attenuated signal, a higher level of acoustic pressure is observed in the frequency range between 50 Hz and 2,000 Hz. In the case of the FFT analysis for HPF filtration shown in Fig. 7b., it can be seen how the number of amplitudes decreases by increasing the actuation frequency. For the attenuation at 50 Hz HPF, compared

to the initial signal (FFT analysis, Fig. 3b.), a significant attenuation of the first two dominant amplitudes (22.4 Hz and 45 Hz) is observed. In this case the level of maximum linear sound pressure was reduced from 12 Pa (initial signal) to 8 Pa.

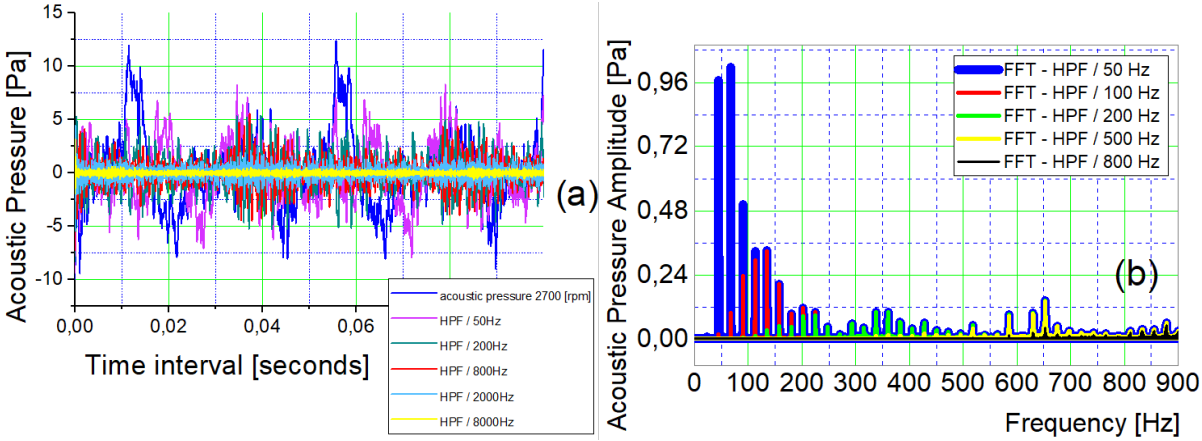

Fig. 7 - HPF attenuation of the initial signal at 2,700 rpm

(a) Acoustic pressure of the signal filtered by HPF at 50 Hz, 200 Hz, 800 Hz, 2,000 Hz and 8,000 Hz
(b) FFT diagram of the signal filtered at 50 Hz, 100 Hz, 500 Hz and 800 Hz HPF

From an auditory point of view, for the attenuation HPF by audio playback of the signal saved in audio format, the perceived noise decreases significantly with the increase of the actuation frequency, especially by the attenuation of low and medium frequencies (20 Hz – 1,600 Hz). For attenuation HPF at 50 Hz, 100 Hz, 200 Hz, 500 Hz and 800 Hz, high-amplitude pulses are completely attenuated, but the perceived noise still contains high-pitched amplitudes that are disturbing to the ear. By attenuation HPF at 1,000 Hz, auditory noise is significantly reduced compared to the initial measured signal but still contains enough amplitudes of medium frequency that are disturbing. By attenuating HPF to 2,000 Hz, the noise has a very low level of sound pressure level being less disturbing auditorily. By attenuating at 5,000 Hz, 8,000 Hz and 10,000 Hz HPF, an almost complete reduction of the unfiltered signal measured at 2,700 rpm was obtained. From the audio playback, the resulting sound has small amplitude, so a significant audio amplification is needed to be able to perceive the difference between the three filters. Above the frequency of 10,000 Hz, the resulting noise can no longer be perceived by the human ear.

OPTIMIZATION OF MEASURED NOISE

According to the analysis performed, it is possible to identify the main frequency ranges containing FFT spectral components producing dominant noise and the physiological effect signaled when playing audio files as follows (Fig. 8.):

- attenuation zone 1 between 0 Hz - 200 Hz
- attenuation zone 2 between 300 Hz - 400 Hz
- attenuation zone 3 between 550 Hz - 700 Hz
- attenuation zone 4 between 900 Hz – 1,050 Hz
- attenuation zone 5 between 2,000 Hz – 25,600 Hz

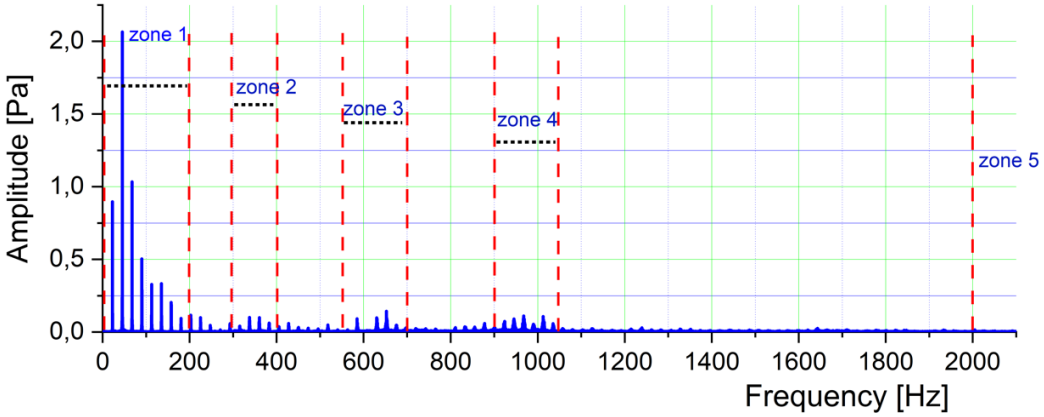

Fig. 8 - FFT diagram of the initial acoustic signal measured at 2700 rpm and filtered frequency areas

Within the acoustic processing software, these attenuation limits were chosen experimentally based on the level of the maximum FFT amplitudes in the low frequency, medium frequency, high frequency range and the specific stamp of the sound resulted from the audio files. In the case of exhaust noise, measured at 2,700 rpm, for this selective attenuation of high amplitude frequency ranges, the following LPF and HPF filters are applied as indicated:

- filtering HPF / 200 Hz and LPF / 300 Hz
- filtering HPF / 400 Hz and LPF / 550 Hz
- filtering HPF / 700 Hz and LPF / 900 Hz
- filtering HPF / 1,050 Hz and LPF / 2,000 Hz

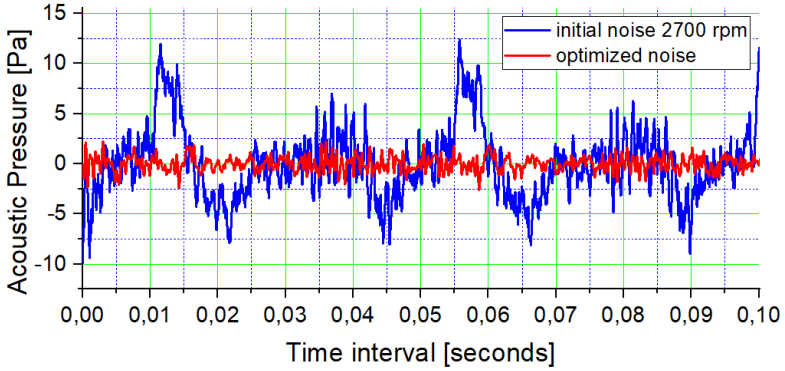

Fig. 9 - Comparison between the acoustic pressure of the initial signal (2,700 rpm) and the signal, optimized by selective filtering (LPF - HPF)

After the filtering, the audio files were generated separately. Final signal from these selective filtering contains all audio files combined (Fig. 9.). Fig. 10a. shows the FFT analysis of the signal attenuated by LPF and HPF compared to the initial signal (FFT analysis, Fig. 3b.). A complete attenuation of amplitudes lower than 200 Hz is observed so the high amplitude pulsations are significantly reduced especially in the low frequency range. The maximum value of the acoustic pressure amplitude of 2 Pa is reduced to 0.1 Pa for optimized signal.

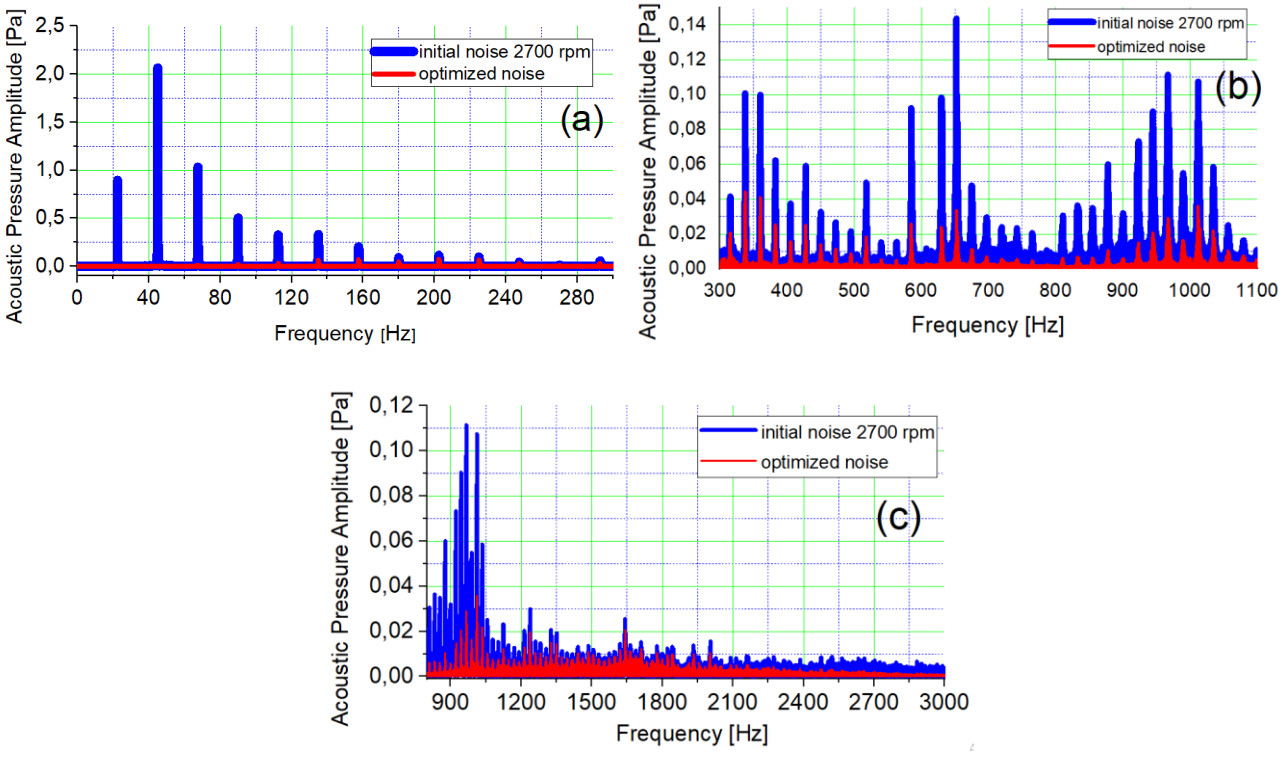

Fig. 10 - Comparison of FFT analysis, initially measured signal and signal optimized by LPF and HPF (2,700 rpm)
(a) frequency range 0 Hz - 300 Hz, (b) frequency range 300 Hz – 1,100 Hz, (c) frequency range 750 Hz – 3,000 Hz

From the FFT analysis for the frequency range 300 Hz – 1,100 Hz (Fig. 10b.), the optimized signal is close in shape to the initial signal but the amplitude level is much lower and the resulting noise is less disturbing auditorily. By audio playback of the attenuated signal, the resulting noise is close to the stamp of the initially measured sound and at a much lower level. The tone of the noise did not change significantly, but its intensity decreased. **Error! Reference source not found.**c. shows the FFT analysis for the 750 Hz – 3,000 Hz frequency range of the attenuated signal / initial signal, where an almost complete attenuation of the high frequency range is observed.

CONCLUSIONS

The result and the audio effect obtained from the acoustic filters can be highlighted only by playing audio files made in waveform audio files format. Following the attenuation and optimization stages, the audio playback of the generated effect is achieved by using an amplifier, a speaker and a sound level meter. According to the experimental optimization, the need to attenuate the measured noise at the exhaust (for this type of engine) for the 20 Hz – 3,000 Hz frequency range is confirmed.

The audio files are generated and processed separately for each type of attenuation applied, resulting in an audio signal containing data values representing the variation of the optimized sound pressure level. The optimization by the selective combination in frequency bands of the low pass filters (LPF) and high pass filters (HPF) was obtained after a total summation of the filtering effects in a single audio file. The main frequency ranges, containing dominant noise generating FFT spectral components in this processing, are presented compared to the initial noise depending on the resulting specific stamp, transmission frequency and amplitude level.

Due to experimental results obtained, the efficiency can be confirmed by the selective combination of the two types of acoustic filters, thus determining the frequency range in which they have an effect. The attenuated frequency range and the optimized method applied require an individual approach depending on the type of internal combustion engine and its operating speed range.

By using this method of analysis, it was possible to make a classification of the attenuation effects generated according to the version of the attenuator chosen in correlation to the analysis of the primary noise supplied / produced by the engine without attenuation system and components. Even if the noise attenuation effects and optimizations in the frequency bands are auditorily similar to the actual situation, it should be specified that in this case the gas flow is considered equal to zero.

It should be noted that the proposed noise attenuation approach technique has an obvious degree of novelty. This method of analysis is less found as research in the literature. This has an obvious applicability in establishing the optimal parameters for the design of noise attenuators. The fact that the audio playback indicated that the stamp of the sound does not change, we suggest, possibly a new applicability regarding the generation of low intensity fake noise inside cars equipped with electric motors to simulate a variation of noise in relation to specific driving conditions.

This function of reproducing a false noise inside electric vehicles could be activated and controlled by the driver, who can choose the specific sound of the internal combustion engine, according to preferences, from a wide range of processed sounds. In this case, the possibilities of selecting and audio playback of sounds specific to internal combustion engines could be unlimited, varying by type of simulated engine, type of simulated vehicle and driving conditions, respectively acceleration, deceleration, engine speed, vehicle speed, engine torque etc.

REFERENCES

[1] Babu, A.R., Amba, P.R., (2014), Simulation of new design muffler to reduce noise in exhaust system of SI engine, *International journal of mechanical and production engineering*, vol.2, no.11, ISSN 2320-2092, pp. 5-9;

[2] Colin, H., Con, D., Kristy, H., (2017), *Fundamentals of acoustics and frequency analysis*, Publishing House Wiley;

[3] Erkan, S., Hakan, A., Burak, B., (2021), A statistical design optimization study of a multi-chamber reactive type silencer using simplex centroid mixture design, *Journal of low frequency noise, vibration and active control*, vol.40(I), SAGE Journals, pp. 626-638;

[4] Fang, J., Zhou, Z., Hu, X., Wang, L., (2009), Measurement and analysis of exhaust noise from muffler on an excavator, *International journal of precision engineering and manufacturing*, vol.10, no.5, ISSN 1392-8716, pp. 59-66;

[5] Filip, N., Candale, L., (2002), Researches regarding the noise conversion from tractor engine in order to reduce the intake manifold noise, (Cercetări de conversie a zgomotului la un motor de tractor pentru a reduce zgomotul din colectorul de admisie), *40th Symposium actual tasks of agricultural engineering*, vol.8, Croatia, ISSN 1333-2651, pp. 311-318;

[6] Filip, N., (2000), *Vehicle noise*, *(Zgomotul la autovehicule)*, Publishing House Todesco, Cluj-Napoca / Romania, ISBN 973-99659-9-7;

[7] Jun, F., Wei, C., Yuan, T., Wenhua, Y., Guangming, L., And Yu, L., (2015), Modification of exhaust muffler of a diesel engine based on finite element method acoustic analysis, *Advances in mechanical engineering*, vol.7, no.4, SAGE Journals, pp. 1-11;

[8] Lee, J. K., Oh, S. K., Lee, J. W., (2020), Methods for evaluating in-duct noise attenuation performance in a muffler design problem, *Journal of sound and vibration*, vol.464, Elsevier, ISSN 0022-460X;

[9] Matthew, H., (2004), *Vehicle refinement controlling noise and vibration in road vehicles*, vol.1, Butterworth-Heinemann, United Kingdom, ISBN 9780080474755;

[10] Mihai, B., Ovidiu, V., (2006), The mufflers modeling by transfer matrix method, (Modelarea atenuatorului de evacuare prin metoda matricei de transfer),*10th WSEAS International conference on applied mathematics*, Dallas, Texas, pp. 476-483;

[11] Mohiuddin, A.K.M., Mohd, R., Shukri, M., (2005), Experimental study of noise and back pressure for silencer design characteristics, *Asian network for scientific information*, vol.5, no.7, ISSN 1812-5662, pp. 1292-1298;

[12] Munjal, M., (2014), *Acoustics of ducts and mufflers*, Publishing House Wiley, ISBN 978-1-118-44312-5;

[13] Myonghyon, H., (2008), *Sound reduction by a Helmholtz resonator*, PhD. Thesis, Lehigh University, Pennsylvania;

[14] Peter, S., Mirko, C., Primoz, L., Jurj, P., (2015), Adaptive muffler based on controlled flow waves, *Journal of the acoustical society of America*, vol.137, no.6, pp. 503-509;

[15] Rossi, F., (2002), Active noise control technique to improve engine efficiency, Energy and environment, centro interuniversitario di ricerca sull'inquinamento e sull'ambiente, pp. 1-12;

[16] Selamet, A., Denia, F.D., Besa, A.J., (2003), Acoustic behavior of circular dual-chamber mufflers, *Journal of sound and vibration*, vol.265, no.5, ISSN 1095-8568, pp. 967-985;

[17] Wael, A, A., (2020), An exact solution for acoustic simulation based transmission loss optimization of double-chamber silencer, *Sound & Vibration*, Tech Science Press, vol.54, no.4, ISSN 1541-0161, pp. 215-224;

[18] Wei, F., Li-Xin, G., (2016), An investigation of acoustic attenuation performance of silencers with mean flow based on three-dimensional numerical simulation, *Shock and Vibration*, Hindawi Publishing Corporation, vol.2, ISSN 1070-9622, pp. 1-12;

[19] Xiang, Y., Yuhui, T., Li, C., Jie, P., (2015), Sub-chamber optimization for silencer design, *Journal of sound and vibration*, vol. 351, no.8, Elsevier, ISSN 0022-460X, pp. 57-67.